ELSEVIER

Development of Methods for Mapping Global Snow Cover Using Moderate Resolution Imaging Spectroradiometer Data

Dorothy K. Hall, George A. Riggs,** and Vincent V. Salomonson†*

An algorithm is being developed to map global snow cover using Earth Observing System (EOS) Moderate Resolution Imaging Spectroradiometer (MODIS) data beginning at launch in 1998. As currently planned, digital maps will be produced that will provide daily, and perhaps maximum weekly, global snow cover at 500-m spatial resolution. Statistics will be generated on the extent and persistence of snow cover in each pixel for each weekly map, cloud cover permitting. It will also be possible to generate snow-cover maps at 250-m spatial resolution using MODIS data, and to study snow-cover characteristics. Preliminary validation activities of the prototype version of our snow-mapping algorithm, SNOMAP, have been undertaken. SNOMAP will use criteria tests and a decision rule to identify snow in each 500-m MODIS pixel. Use of SNOMAP on a previously mapped Landsat Thematic Mapper (TM) scene of the Sierra Nevadas has shown that SNOMAP is 98% accurate in identifying snow in pixels that are snow covered by 60% or more. Results of a comparison of a SNOMAP classification with a supervised-classification technique on six other TM scenes show that SNOMAP and supervised-classification techniques agree to within about 11% or less for nearly cloud-free scenes and that SNOMAP provided more consistent results. About 10% of the snow cover, known to be present on the 14 March 1991 TM scene covering Glacier National Park in northern Montana, is obscured by dense forest cover. Mapping snow cover in areas of dense forests is a limitation in the use of this procedure for global snow-cover mapping. This limitation, and sources of error will be assessed globally as SNOMAP is refined and tested before and following the launch of MODIS.

*Hydrological Sciences Branch, Laboratory for Hydrospheric Processes, NASA / Goddard Space Flight Center, Greenbelt, MD
**Research and Data Systems Corporation, Greenbelt, MD
†Earth Sciences Directorate, NASA / Goddard Space Flight Center, Greenbelt, MD

Address correspondence to Dr. Dorothy K. Hall, NASA Goddard Flight Center, Code 974, Greenbelt, MD 20771.
Received 9 February 1995, accepted 13 May 1995.

INTRODUCTION

The highly reflective nature of snow combined with its large surface coverage (snow can cover up to 40% of the Earth's land surface during the Northern Hemisphere winter), make snow an important determinant of the Earth's radiation balance (Foster and Chang, 1993). Snow on the ground influences biological, chemical, and geological processes (Walsh et al., 1985; Robinson and Kukla, 1985; Allen and Walsh, 1993; Robinson et al., 1993). Many areas of the world rely on snowmelt for irrigation and drinking water and must monitor snowpacks closely throughout the winter and spring for assessment of water supply (Carroll et al., 1989).

Snow cover is a key component of regional and global climate, and it is vital to have an accurate and long-term database established on snow-extent variability. General circulation models (GCMs) do not simulate the present Arctic climate very well (Bromwich and Tzeng, 1994), and thus improvements in the measurement of global snow cover and other cryospheric elements are key to improving the GCMs.

The Moderate Resolution Imaging Spectroradiometer (MODIS) will be launched as part of the first Earth Observing System (EOS) platform in 1998 with a capability to study geophysical features globally (Salomonson and Toll, 1991), including mapping the areal extent and reflectance of global snow cover on a daily basis. A prototype algorithm, called SNOMAP, is currently being developed using TM data to enable automated mapping of areal extent of snow cover using future MODIS data.

Efforts to develop and refine SNOMAP, and to assess its accuracy, are discussed in this paper. Examples of work on algorithm development from Landsat thematic mapper (TM) scenes acquired over northern Montana (including Glacier National Park); the Chugach Mountains, Alaska; Glacier Bay, Alaska; northern Minnesota; and the Sierra Nevada Mountains, California in

REMOTE SENS. ENVIRON. 54:127–140 (1995)

655 Avenue of the Americas, New York, NY 10010

0034-4257 / 95 / $9.50
SSDI 0034-4257(95)00137-P

the United States, and an area in southeastern Iceland are presented.

BACKGROUND

Satellite sensors have been employed to map snow cover, and to measure (or estimate) snow depth and reflectance. Using satellite data, available since 1966, it has been shown that there is an inverse relationship between hemisphere-averaged, monthly mean snow cover, and temperature fluctuations (Robinson and Dewey, 1990; Robinson et al., 1991; Gutzler and Rosen, 1992; NOAA, 1994). National Oceanic and Atmospheric Administration (NOAA) satellite data including the Advanced Very High Resolution Radiometer (AVHRR) enable the measurement of snow extent using visible, near-infrared and thermal-infrared sensors at a resolution of about 1 km (Matson et al., 1986; Matson, 1991). NOAA snow charts are digitized weekly using the National Meteorological Center's standard-analysis grid, an 89×89 cell Northern Hemisphere grid with polar-stereographic projection. Cell resolution ranges from 16,000–42,000 km^2. Only cells with a least 50% snow cover are mapped as snow (Robinson et al., 1993).

Other snow-mapping studies are performed on regional and local scales using ground-based measurements, NOAA AVHRR, Landsat multispectral scanner (MSS) and TM data, and aircraft data (for example, see Carroll, 1990; Rango, 1993). Regional snow products are produced in >4000 drainage basins in the western United States and Canada on a weekly basis during the snow season using NOAA AVHRR 1-km data (Carroll, 1990; Rango, 1993). Use of passive-microwave sensors on board the Nimbus -5, -6, and -7 satellites and the Defense Meteorological Satellite Program (DMSP) satellite has allowed successful measurement of snow extent at a 25 to 30-km resolution through cloud cover and darkness since 1978.

The Landsat MSS and TM sensors may be used for measurement of snow-covered area over drainage basins (Rango and Martinec, 1982). AVHRR data have also been used successfully to measure snow at the drainage-basin scale. The 16-day repeat cycle of the Landsat-4 and -5 satellites, however, coupled with the potential for cloud cover, precludes the use of Landsat data for operational snow mapping. Additionally, Landsat TM data are useful for the quantitative measurement of snow reflectance (Dozier et al., 1981; Dozier, 1984, 1989; Hall et al., 1992; Winther, 1992).

Various techniques, ranging from visual interpretation, multispectral image classification, decision trees, change detection, and ratios (Kyle et al., 1978; Bunting and d'Entremont, 1982), have been used to map snow cover with remotely sensed data (see, for example, Rango, 1975). Additionally, spectral-mixture modeling has been demonstrated as an important new technique for subpixel classification of snow in a scene (Nolin et al., 1993; Rosenthal, 1993).

DESCRIPTION OF THE MODIS SENSOR

The Moderate Resolution Imaging Spectroradiometer is an imaging radiometer that uses a cross-track scan mirror and collecting optics, and a set of individual detector elements to acquire imagery of the Earth's surface and clouds in 36 discrete spectral bands. MODIS is scheduled for launch as a facility instrument of the EOS polar-orbiting platform in 1998. The primary purpose of MODIS data is to permit the regional to global study of the land, atmosphere, and ocean on a daily or near-daily basis (Salomonson et al., 1992). Key land science objectives are to study global vegetation and ground cover, global land surface change, vegetation properties, surface albedo, surface temperature, and

Table 1. MODIS Band Number (#), and Bandwidths in μm

MODIS band #	*bandwidth*	*band #*	*bandwidth*
1	0.620–0.670	19	0.915–0.965
2	0.841–0.876	20	3.66–3.84
3	0.459–0.479	21	3.93–3.99
4	0.545–0.565	22	3.93–3.99
5	1.230–1.250	23	4.02–4.08
6	1.628–1.652	24	4.43–4.50
7	2.105–2.155	25	4.48–4.55
8	0.405–0.420	26	1.36–1.39
9	0.438–0.448	27	6.54–6.90
10	0.483–0.493	28	7.18–7.48
11	0.526–0.536	29	8.40–8.70
12	0.546–0.556	30	9.58–9.88
13	0.662–0.672	31	10.78–11.28
14	0.673–0.683	32	11.77–12.27
15	0.743–0.753	33	13.19–13.49
16	0.862–0.877	34	13.49–13.79
17	0.890–0.920	35	13.79–14.09
18	0.931–0.941	36	14.09–14.39

Table 2. TM Band Number (#), and Bandwidths in μm

TM band #	*bandwidth*
1	0.45–0.52
2	0.52–0.60
3	0.63–0.69
4	0.76–0.90
5	1.55–1.75
6	10.40–12.50
7	2.08–2.35

snow and ice cover and characteristics (Salomonson et al., 1992; Running et al., 1994).

Spatial resolution of the MODIS sensor at nadir varies with spectral band and is 250, 500, or 1000 m. The spectral bands cover parts of the electromagnetic spectrum from about 0.4–14.0 μm (Table 1), thus spanning the visible and thermal-infrared parts of the spectrum. MODIS bands covering visible, near-infrared and short-wave infrared parts of the spectrum will be used in the snow-mapping algorithm. On the first EOS platform, MODIS is scheduled to have a morning (10:30 A.M. ± 15 min) overpass (descending mode platform). Further details about the MODIS instrument characteristics can be found in Salomonson and Barker (1992) and King et al. (1992).

The wide swath (± 55°) of the MODIS sensor will be suitable for large-area coverage. Only data from ± 45° will be used for production of the snow maps because the distortions in pixel geometry and the increases in snow anistropy at angles greater than ± 45° are likely to adversely affect our ability to calculate snow-covered area using SNOMAP. Even with this restriction, at a scan angle of ± 45°, virtually all seasonally snow-covered areas can be imaged daily (Fleig et al., in press).

MODIS band selection for SNOMAP has been largely determined by research done with comparable wavelength data from the TM sensors. TM bands are listed in Table 2. MODIS Airborne Simulator (MAS) data will increasingly be used to refine SNOMAP. As MAS are acquired and analyzed, selection of optimum MODIS bands to use in SNOMAP may change in the prelaunch time frame.

Snow typically has very high visible reflectance, and based on MODIS specifications, MODIS band 4 should not saturate if snow is present, thus it is a good band for snow measurement and identification. This is an important advance as saturation in some AVHRR channels and TM bands has been a problem over snow-covered areas.

RESULTS

Description of the SNOMAP Algorithm for Mapping Snow Cover

SNOMAP (Riggs et al., 1994) is an algorithm designed to identify snow, if present, in each MODIS pixel each day. As currently planned, if snow is present in any pixel on any day during the compositing period, that pixel will be considered to be snow covered. There will be a daily and perhaps a weekly snow-cover product.

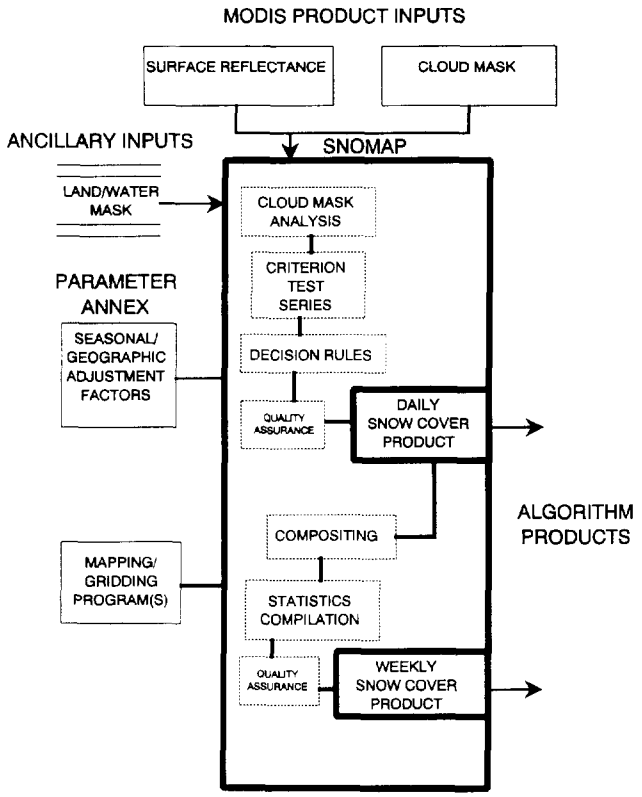

Figure 1. A conceptual flow diagram for SNOMAP.

In the context of the Earth Observing System Data Information System (EOSDIS), it is expected that surface reflectance and a cloud mask produced by other MODIS investigators will be used as input to SNOMAP (Fig. 1). When SNOMAP is implemented globally, using MODIS data, a land/water mask will also be used. Seasonal and geographic adjustments will be made to the algorithm, and mapping/gridding programs will be employed to generate the global snow-cover data product. A daily and weekly snow-cover data product, and statistics on snow-cover persistence for the weekly product are the outputs of SNOMAP. Areas that are covered by persistent cloud cover will be identified as such. Cloud-cover considerations will be discussed further in a later section.

Unique aspects of the MODIS-derived global snow maps include: fully automated production, anticipated improved spectral discrimination between snow and other features, relative to what is available today, and statistics describing snow-cover persistence in each pixel of the weekly product.

Landsat TM data are used as a surrogate for some of the spectral bands of MODIS in order to develop an algorithm to map snow using future MODIS data. For

initial algorithm-development efforts, TM data are better suited to represent MODIS data than are any other satellite data for simulation of spectral characteristics that apply to mapping snow cover. There are important differences between the TM and MODIS data that make the use of TM data alone inadequate to simulate MODIS data, however. First, the TM data have a pixel resolution of 30 m whereas the MODIS pixel resolution will be 250 m to 1 km. The finer resolution of the TM data is suitable for mapping snow in drainage basins, whereas the MODIS 250-m–1-km resolution is suitable for regional- and global-scale snow mapping as well as for mapping snow in drainage basins. There are fewer TM bands than there are MODIS bands, and the MODIS and TM band widths differ. Also, because the TM sensor has only one band in the thermal-infrared part of the spectrum (TM band 6), it is difficult to determine the potential utility of the MODIS thermal-infrared bands, using TM data alone. Data from other sensors, such as the MAS, and the AVHRR, are also being used in development efforts.

At-satellite reflectance is calculated using the following equation (Markham and Barker, 1986) in our prototype algorithm,

$$\rho_p = (\pi L_\lambda d^2)/(ESUN_\lambda \cos\theta_s) \quad (1)$$

where:

ρ_p = unitless effective at-satellite planetary reflectance;
L_λ = spectral radiance at sensor aperture ($mWcm^{-2}sr^{-1}\mu m^{-1}$);
d = Earth–Sun distance (Astronomical Units);
$ESUN_\lambda$ = mean solar exoatmospheric irradiance ($mWcm^{-2}\mu m^{-1}$);
θ_s = solar zenith angle (degrees).

Because the above formulation assumes isotropy of the surface, and snow is an anisotropic reflecting surface, there is an inherent error in the reflectance value calculated using this technique. The error will be smaller for freshly fallen snow than for older, metamorphosed snow, because fresh snow can be nearly an isotropic reflecting medium (Steffen, 1987). This error is expected to be small enough so that SNOMAP results should not be altered significantly, if at all, by this source of error.

Use of Reflectances versus Digital Numbers

Because the same DN values on different TM scenes are likely to correspond to different reflectances, the use of reflectances improves the identification of snow because reflectance is based on fraction of incoming solar radiation, and the cosine effect of sun angle on incident radiation is accounted for. Thus, optimum detection of snow cover requires that data be expressed in physical units, for example, reflectance. MODIS calibrated, geolocated, atmospherically corrected radiances are the planned input data for SNOMAP.

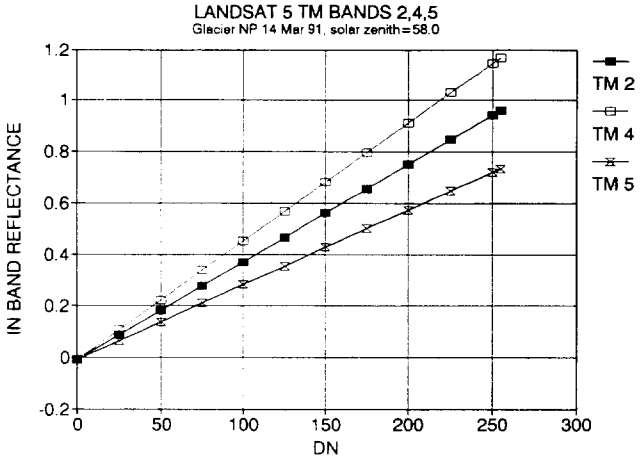

Figure 2. Relationship between digital number (DN) and reflectance on the 14 March 1991 TM scene covering Glacier National Park, Montana. Reflectance was calculated using formulation by Markham and Barker (1986).

In order to test the assumption that the use of reflectances is better than the use of DNs for snow-cover mapping, a study was conducted using two TM scenes in northern Montana: 14 March 1991 and 06 March 1994, to identify snow cover. The relationship between the DN and reflectance values for the 14 March 1991 TM scene covering Glacier National Park is shown for 3 TM bands in Figure 2. Sensor saturation is common in TM bands over snow and no further information can be derived from reflectance once saturation has occurred. Both DNs and reflectances were used to calculate the Normalized Difference Snow Index (NDSI). The NDSI is an integral part of the SNOMAP algorithm for the identification of snow:

$$\text{NDSI} = \frac{(\text{TM band 2} - \text{TM band 5})}{(\text{TM band 2} + \text{TM band 5}).} \quad (2)$$

Having its heritage with the the Normalized Difference Vegetation Index (NDVI) (Tucker, 1979, 1986), and band-rationing techniques (Kyle et al., 1978; Bunting and d'Entremont; Dozier, 1984), the NDSI is used to identify snow in an automated-algorithm environment. The utility of the NDSI is based on the fact that snow reflects visible radiation more strongly than it reflects radiation in the middle-infrared part of the spectrum. Because the reflectance of clouds remains high in the region of the spectrum in which TM band 5 is located, and the reflectance of snow drops to near-zero values, the NDSI also functions as a snow / cloud discriminator.

A greater snow cover was calculated when reflectances were used to calculate the NDSI versus when DNs were used, and ground-truth measurements simultaneous with the 14 March 1991 data acquisition indi-

Table 3. Comparison of the Number of Snow-Covered Pixels (and Percentage of Scene that Was Snow Covered) Calculated Using DNs and Reflectances (R) to Calculate the NDSI

14 March 1991	*06 March 1994*
DN method 10,272,700 (25.7%)	9,733,780 (23.4%)
R method 13,483,976 (32.4%)	13,088,391 (31.5%)

cated that the larger amount of snow cover was more accurate (Table 3).

In testing snow-covered areas using TM scenes in the United States (Alaska, California, Montana, and Minnesota), and Iceland, NDSI values greater than or equal to approximately 0.4 were found to represent snow cover well, and to separate snow from most clouds. This was also found to be an effective threshold for snow mapping in the Sierra Nevadas by Dozier (1989). Sensitivity of individual criteria tests can be studied by changing the threshold value incrementally and analyzing the effect on results. These results reveal that there is not an exact NDSI threshold for snow, but that a credible threshold for snow mapping can be established.

For six TM scenes, the NDSI threshold value for snow was increased incrementally from 0 to 1.0 in steps of 0.05 as shown in Figures 3a and 3b. If a pixel had an NDSI value equal to or greater than the threshold, it was identified as snow. Results are expressed as total number of snow pixels for a threshold as shown in Figure 3a, and as change in snow cover between successive NDSI thresholds as shown in Figure 3b.

A consistent observation is that the areal extent (number of snow pixels) decreases as the NDSI threshold was increased from 0 to 1.0 (Figure 3a). The amount of change between thresholds varied from relatively constant to rapid depending on the particular scene and threshold. Those results indicate that a range of NDSI threshold values between 0.10 and 0.50 produces consistent results among images, with only small changes in snow cover between adjacent thresholds as shown in Figure 3b. Generally a 10% or less change in snow cover was observed between successive thresholds over the NDSI range of 0.10 to 0.50 for all scenes studied. NDSI threshold values greater than 0.50 resulted in large changes in snow extent; visual analysis indicated that actual snow cover was eliminated at these higher thresholds. At low NDSI thresholds, that is 0.20 and lower, many non-snow pixels are identified as snow. Acceptable snow cover results have been found with NDSI thresholds in the range of 0.25 to 0.45.

Water bodies may have NDSI values in the range of those for snow, however, water has a lower near-infrared reflectance and can thus can be distinguished from snow. In SNOMAP, as in previous work (Dozier, 1989), an additional test for snow must be conducted after the NDSI is calculated. In order to be mapped as snow in SNOMAP, the TM band 4 reflectance must be $>11\%$. A pixel is classified as snow covered if results of both the NDSI and reflectance tests lie within the intersection of

Figure 3. (a) In this figure, the total number of snow pixels at each NDSI threshold is mapped in different TM scenes. GNP refers to a 14 March 1991 scene of northern Montana, including Glacier National Park; Glacier Bay refers to a 6 October 1992 scene covering Glacier Bay in southeastern Alaska; Sierra refers to a 10 May 1992 scene covering the Sierra Nevada Mts. in California; Minn refers to a 9 March 1985 scene covering part of northern Minnesota; Vatna refers to a 19 October 1992 scene of southeastern Iceland including Vatnajökull, an ice cap; Chugach refers to a 29 September 1992 scene of the Chugach Mts., in southern Alaska. (b) In this figure, the change in snow cover mapped is shown at each NSDI threshold value. Note that small changes in amount of snow cover mapped occur until a Normalized Difference Snow Index (NDSI) value of about 0.45 is reached.

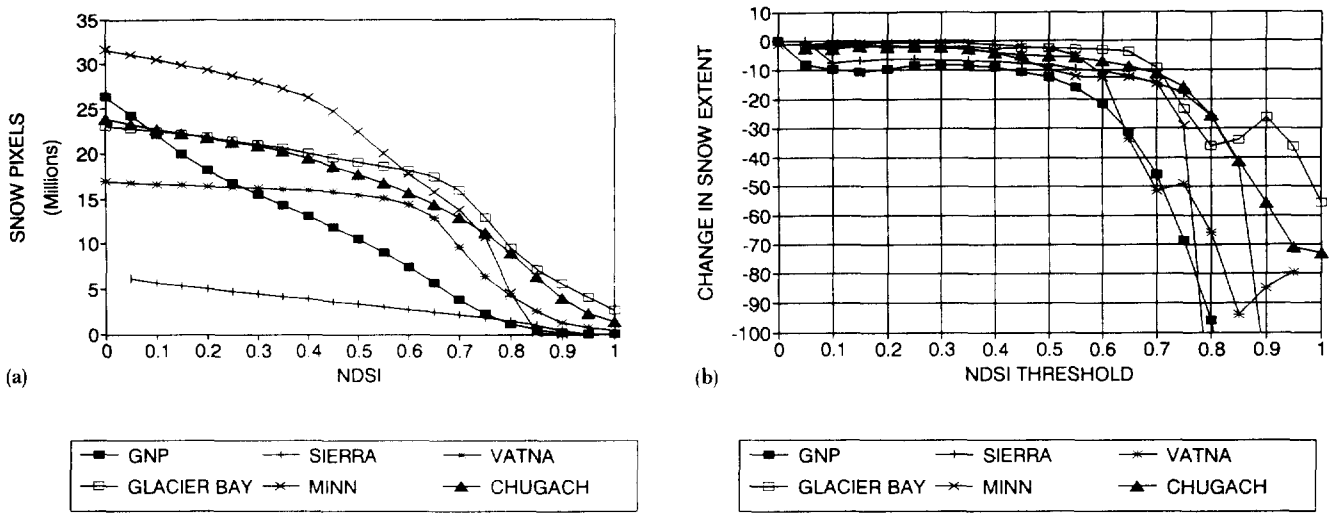

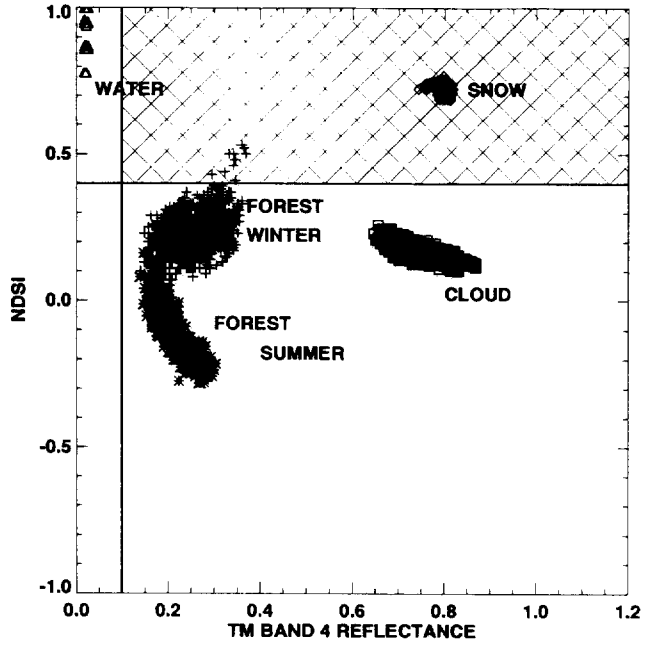

Figure 4. Snow decision region for SNOMAP criteria tests. Thresholds for TM band 4 reflectance and NDSI tests are the solid lines. Pixels falling in quadrant one of the plane formed by the intersection of the threshold lines (shaded area) are identified as snow. Data are from TM scenes of Glacier National Park, Montana: 14 March 1991 (for snow, $n = 2000$; for cloud, $n = 10{,}000$; for snow-covered forest, $n = 1750$); and 03 September 1990 (for forest with no underlying snow, $n = 1050$, for water, $n = 1750$). Scene identification numbers for the 14 March 1991 and 03 September 1990 TM scenes, respectively, are # 5256917454 and # 5237717441.

the acceptance regions of these criteria tests (see hatched area on Figure 4). Pure pixels of water, forest, cloud, and snow were selected to show separation of features. Also shown are pixels from a snow-covered forest in Glacier National Park, Montana from the 14 March 1991 TM scene. The snow-covered forest selected was the same area (west of Lake Mc Donald) as selected for pure forest cover from the 03 September 1990 Glacier National Park scene. Most of the snow-covered forest is not classified as snow by SNOMAP as seen in Figure 4. Adjusting the NDSI threshold downward would permit more snow in forests to be mapped as snow, but, in doing so, non-snow pixels may also be mapped. This illustrates the problem inherent in the thresholding techniques, and will be addressed further as the snow-cover algorithm evolves.

Figures 5a and b show a TM band 5, 4, 2 false-color composite of northern Montana including Glacier National Park (14 March 1991), and the results of SNOMAP on that scene, respectively. Note that in addition to mapping bright, sunlit snow, SNOMAP identifies some snow in mountain and cloud shadows and in forested areas. SNOMAP correctly identifies most or all clouds as non-snow features. Also, the non-snow-covered plains in the northeastern part of the image, which were largely snow-free at the time of image acquisition, are identified correctly as non-snow covered. The snow-covered features in that part of the image are snow- and ice-covered lakes. Similar results have been obtained on all the TM data we have studied so far, including other scenes in the United States (northern Montana, and scenes in northern Minnesota, the Chugach Mountains, Alaska; Sierra Nevada Mountains, California), Antarctica, southeastern Iceland, and the east coast of Greenland. We are continually seeking to identify scenes on which SNOMAP does not accurately represent snow cover in order to improve the algorithm in the pre-launch time frame.

Cloud Cover Considerations

SNOMAP is capable of separating most clouds and snow. Cumulus clouds are generally readily distinguished from snow because the reflectance of cumulus clouds remains high in the region of the spectrum from 1.55–1.75 μm (TM band 5), whereas the reflectance of snow drops. The reflectance of cirrus clouds, however, may not be as high in this region of the spectrum if they are thin and if the reflectance from the ground cover beneath the cloud is visible through the cloud. SNOMAP has been run on TM scenes with cirrus clouds and results are mixed; sometimes the cirrus clouds are identified as clouds and other times they are confused with snow. We do not yet know at what optical thickness the clouds become opaque in TM band 5.

There may be areas in which cloud cover is so prevalent that no useful snow data will be acquired in a given week due to cloud cover. Rossow (1993) has mapped global cloud amount by latitude and season. In his analysis, very few areas are either completely cloudy or completely clear over a 30-day period. He emphasizes, however, that the results in the polar regions probably miss significant amounts of cloudiness because of the difficulty in separating snow and clouds. During the EOS era, with the development of global cloud-cover maps from MODIS, and the global snow and sea ice-cover maps, we will gain a better understanding of the cloud persistence in the polar regions.

ERRORS

Assessment of the inherent errors in hemispheric-scale snow-cover mapping has been difficult (Robinson et al., 1993). Also, the inability to map snow through dense forests is an important limitation in the use of satellite data for mapping snow. Errors are inherent in the calculation of snow-covered area due to several factors. Errors

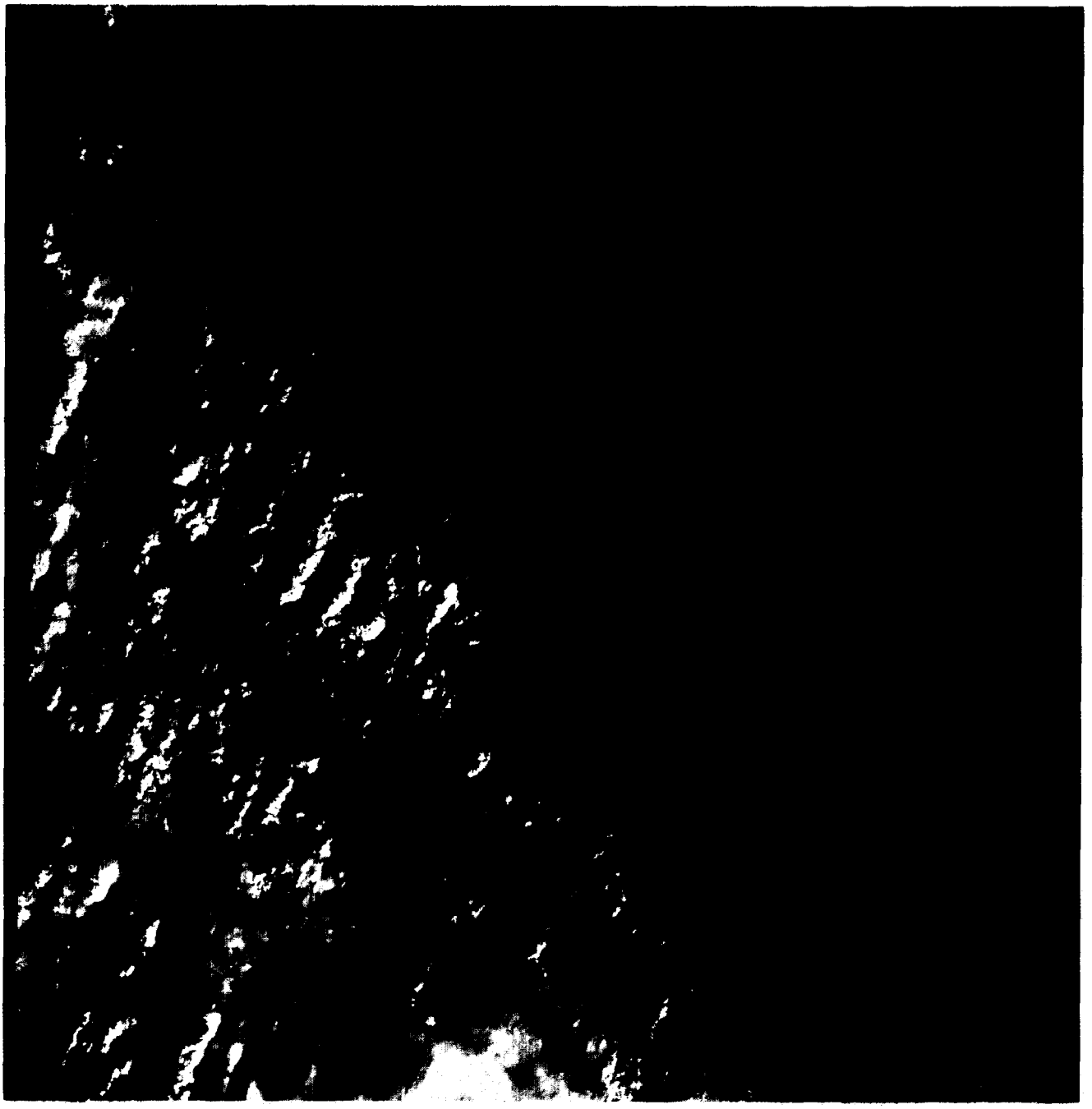

Figure 5. (a) TM band 5, 4, 2 color composite of northern Montana including Glacier National Park, 14 March 1991 (i.d.# 5256917454).

may be caused by the presence of clouds using satellite data from the optical part of the electromagnetic spectrum; smaller errors due to cloud and mountain shadows are also often present. Additionally, errors due to the effects of topography can be large because satellite data depict a flat surface and do not permit areal snow cover to be mapped on mountain slopes; without the use of a digital elevation model, snow-covered area can be greatly underestimated in mountainous areas (Hall et al., in press).

Other sources of error in mapping snow cover using SNOMAP are to be expected due to the inability to map snow that covers less than 60% of a pixel without mapping bright, non-snow features elsewhere in the image. Furthermore, if there are any inaccuracies in the input products, that is, inaccuracy in the calculation

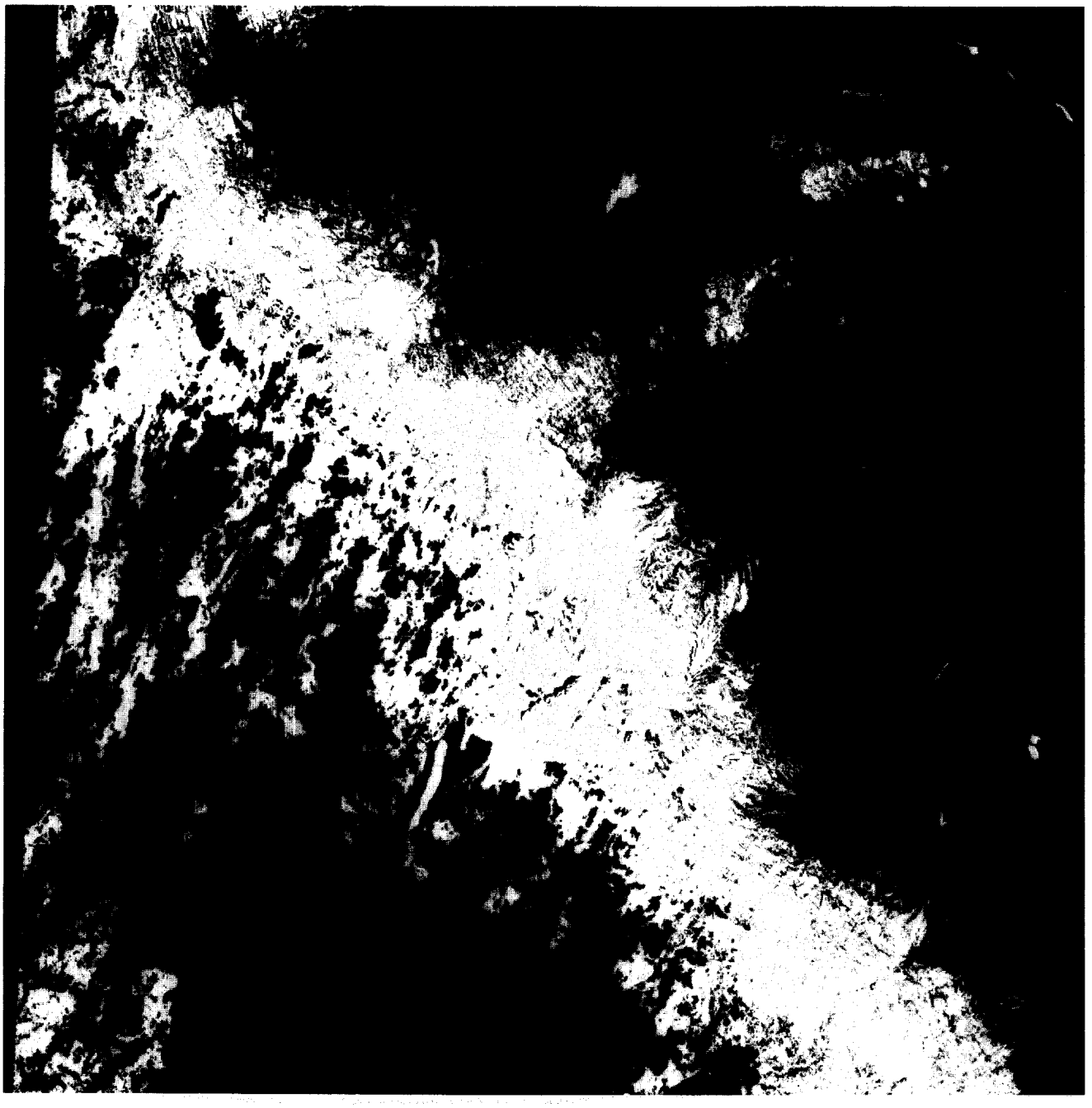

Figure 5. (b) Result of applying the SNOMAP algorithm to image in 5a; white represents snow cover and black represents non-snow-covered areas including clouds.

of the atmospheric correction, this may cause errors in the amount of snow that is mapped by SNOMAP.

Limitations Association with Analysis of Snow Cover in Forested Areas

The presence of dense forests has long been a source of difficulty in snow mapping from aircraft and satellites (Tiuri and Hallikainen, 1981; Foster et al., 1991). Rather than considering this an error, it is probably better deemed a limitation to automated, global snow-cover mapping because the presence of dense forests masks snow cover on the forest floor. Using passive-microwave data, it is also difficult to map snow under dense forests (for example, see Hallikainen et al., 1988; Goodison et al., 1986; Foster et al., 1994). Various models have been developed to permit more snow to be detected under trees using passive-microwave data (Hall et al., 1982; Chang et al., 1992a), however, the problem remains.

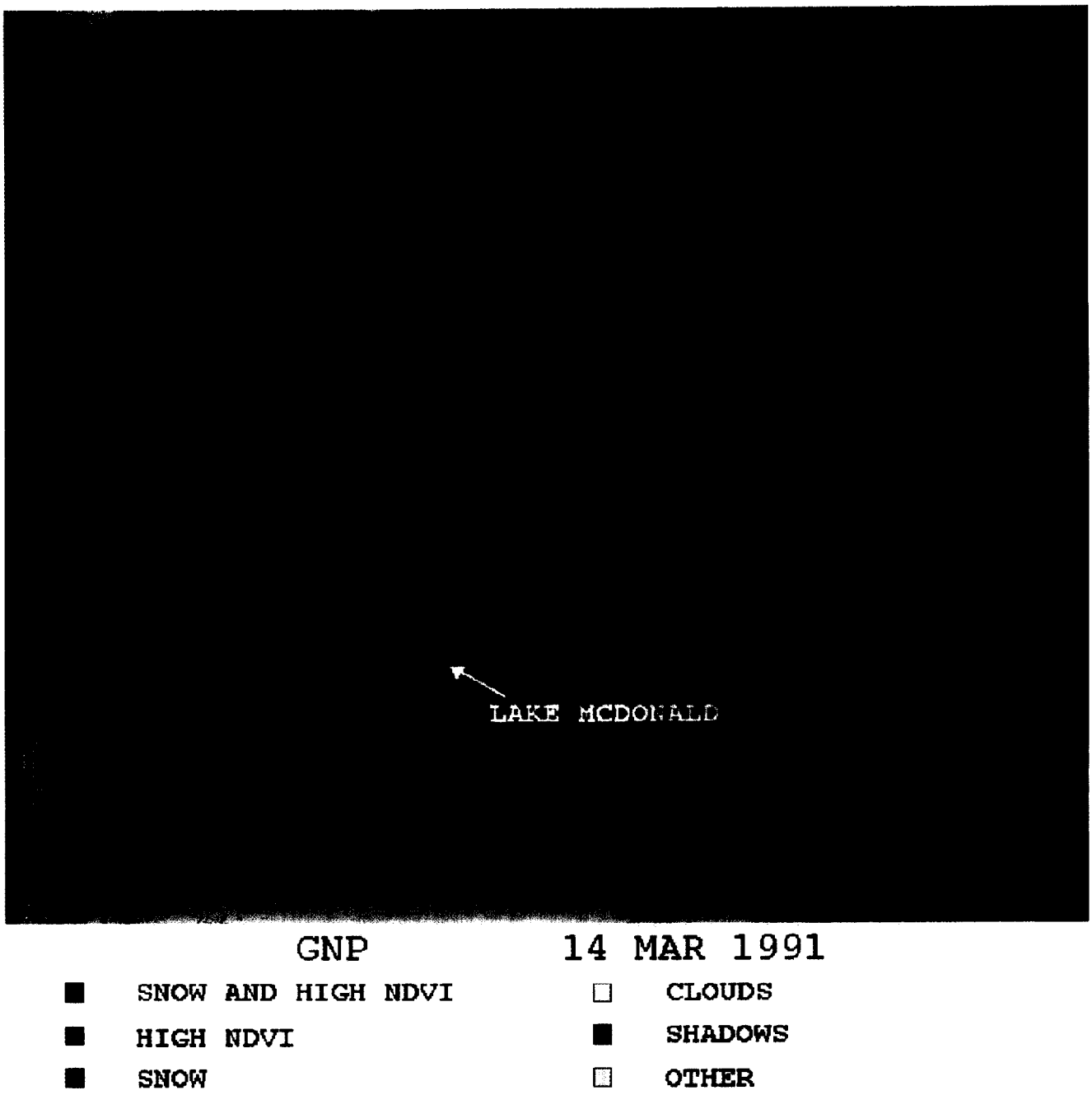

Figure 6. Results of applying the Normalized Difference Vegetation Index (NDVI) to a subscene of the 14 March 1991 TM scene covering part of Glacier National Park, Montana (i.d. # 5256917454). Blue depicts snow cover, dark green depicts areas of high NDVI for which snow cover was not mapped, red depicts snow cover mapped in areas of high NDVI, and white, grey and yellow depict cloud cover. Light-green areas represent non-snow-covered areas. Note the high Normalized Difference Vegetation Index values around Lake Mc Donald.

Analysts using NOAA data to derive Northern Hemisphere weekly snow-cover maps assume a complete snow cover beneath dense forests if the surrounding areas are observed to be snow covered. Using an automated-algorithm approach, it cannot be determined whether snow persists (and for how long) underneath the forest canopy once snow in adjacent areas melts. Because of the uncertainty of assuming snow cover in an automated-algorithm environment at certain times of the year, the MODIS snow-mapping algorithm will not, at least initially, contain code that checks for snow cover in forested areas adjacent to snow-covered areas for the daily snow-cover product, because this could introduce errors and inconsistent results between years.

The weekly snow-cover product will be used to develop a maximum snow-extent map that will show the maximum position of the continental snowline for that week. In doing so, snow cover under forested areas will be mapped.

Using the 14 March 1991 TM scene of northern Montana (covering Glacier National Park), dense forests are defined as places where the NDVI is high (Fig. 6). The NDVI has a close relationship with the photosynthetic capacity of specific vegetation types (Tucker, 1979; Townshend et al., 1993). The theoretical range of the NDVI is -1 to $+1$, but in practice it varies from 0.03 for water to 0.05 for deserts, to 0.6 for areas with the highest levels of photosynthetic activity (Townshend et al., 1993). The NDVI may be calculated using TM data as follows:

$$\text{NDVI} = \frac{(\text{TM band 4} - \text{TM band 3})}{(\text{TM band 4} + \text{TM band 3})} \quad (3)$$

An area of dense forest just west of Lake Mc Donald has an average NDVI of about 0.54 in the 03 September 1990 TM image. The same area has an average NDVI of 0.38 in the 14 March 1991 TM image when snow was present under the forest canopy. In areas of dense forests such as the area near Lake Mc Donald, however, snow under the canopy is not consistently identified by SNOMAP in the March scene. In fact, 10% of areas of dense forests were not identified as snow covered by SNOMAP even though simultaneous field measurements revealed a complete snow cover. Those areas where the average NDVI was high (about 0.38), and no snow is mapped, are shown in green on Figure 6; areas where the average NDVI is high and snow is mapped, are shown in red. Thus SNOMAP permits the mapping of some, but not all snow cover in densely forested areas. The circumstances under which snow is mapped under dense forests will be investigated further.

VALIDATION OF SNOWMAP

Comparison with a Spectral-Mixture Modeling Technique

As part of the validation activities and to determine its accuracy for individual TM scenes, SNOMAP results have been compared with the results from a subpixel snow-cover mapping technique (Rosenthal, 1993). Rosenthal used spectral-mixture modeling and decision trees to map fractional snow cover on a 10 May 1992 TM scene covering part of the Sierra Nevada Mountains, California; ground-truth measurements and aerial photographs were used for validation. Fractional snow-cover classes derived from the spectral-mixture modeling range from 100% snow covers, to 0% snow covers, with intermediate classes containing mixtures of snow, vegetation and rock (Rosenthal, 1993).

Based on comparison with Rosenthal's results, SNOMAP is 98% accurate in identifying pixels covered at least 60% by snow in the 10 May 1992 TM scene of the Sierra Nevada Mountains. Rosenthal's results showing pixels covered 60% or more by snow, and the SNOMAP result, are shown in Figure 7.

Comparison with a Supervised-Classification Technique

Additionally, supervised classification was performed on 6 TM scenes. The results of the supervised classifications were then compared with the results of the SNOMAP classification. Results of each were also later compared interactively with a TM band 5, 4, 2 digital reflectance image of each scene.

Detailed analysis of each scene indicated that, overall, a better classification was performed using SNOMAP than with the supervised classification. Also, SNOMAP did a more consistent job in the snow classifications than was done with supervised classification. In the four nearly cloud-free images, supervised versus SNOMAP results compared well; results of the two classification techniques compared less well in the two scenes (GNP 14Mar91 and Ch 29Sep92) where cloud cover was a significant factor as discussed below (Table 4).

In the case of the 14 March 1991 Glacier National Park scene comparison, because of extensive cloud cover, the supervised classification provided poor results. The supervised classification found 39.3% less snow cover than did the SNOMAP classification (Table 4). Also, using supervised classification, it was difficult to define pixels in cloud shadows that were snow-covered without inadvertently mapping non-snow pixels. In the case of the 29 September 1992 Chugach Mts. scene, a cirrus cloud in the northeastern part of the image was mapped erroneously as snow by SNOMAP, but not by the supervised-classification technique. The supervised classification technique found 19.8% less snow cover in this scene as compared to the SNOMAP classification technique (Table 4). This is because in the supervised classification, the cirrus cloud was selected as a unique feature and mapped accordingly.

SNOMAP mapped areas of shadowed snow much better than did the supervised classification, although in some cases (e.g., the Glacier National Park scene acquired on 09 May 1994), the supervised classification mapped more snow at the edges of snow-covered areas. Both techniques mapped a few, stray, non-snow pixels outside of the snow-covered areas. SNOMAP mapped more snow in dense forests (e.g., around Lake Mc Donald on the 14 March 1991 Glacier National Park scene) than did the supervised classification. Interestingly, SNOMAP did not map very dark glacier ice as snow on the Iceland scene covering Vantnajökull ice cap, whereas the supervised-classification technique did. Using either

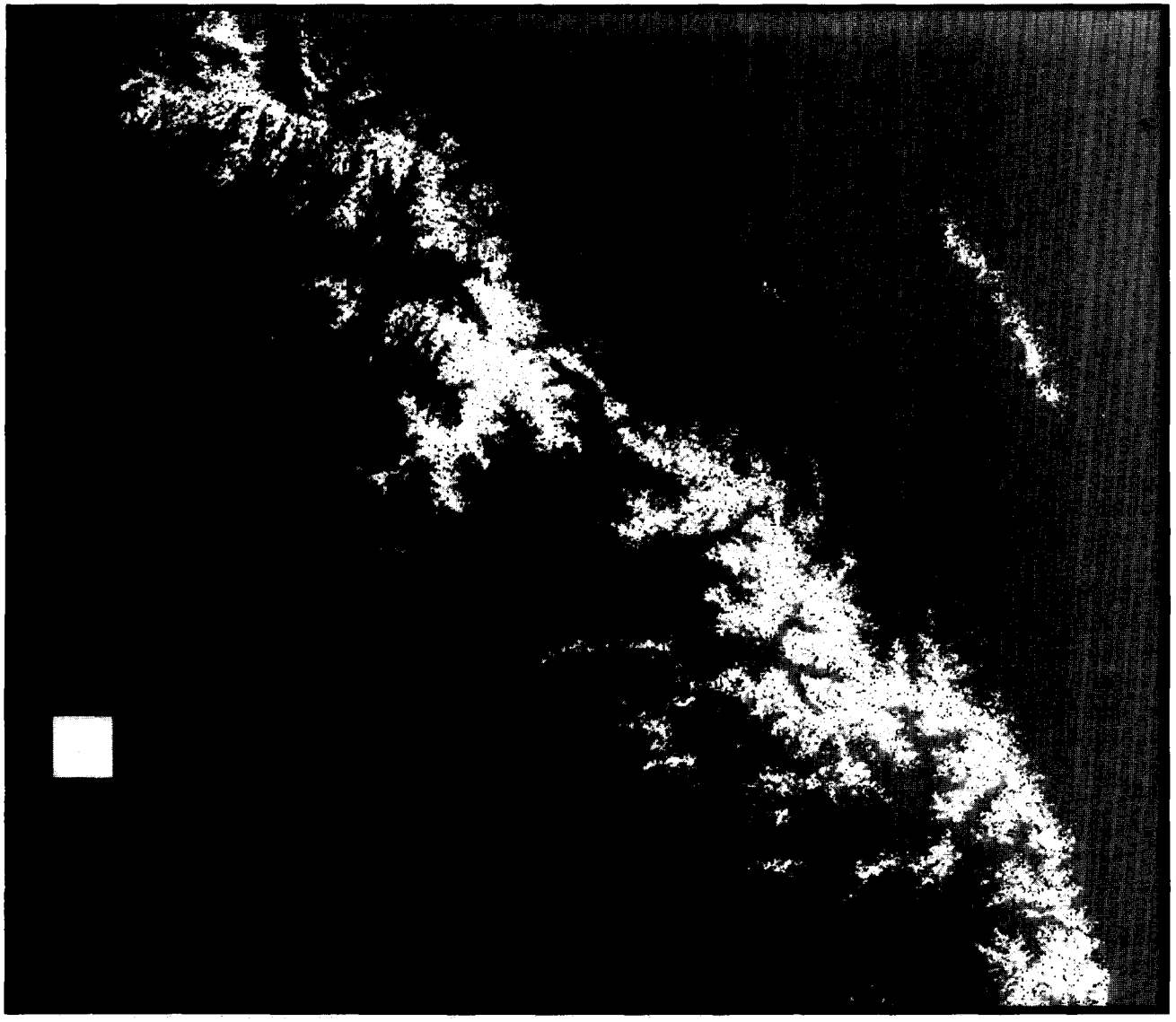

Figure 7. Comparison of results of mapping snow on the 10 May 1992 TM scene (i.d. # 5299217572) of the Sierra Nevadas in California using results from Rosenthal's (1993) spectral-mixture modeling technique, with SNOMAP results.

technique, when there is insufficient signal from the snow, as in the case of completely shadowed pixels, or pixels under a dense tree canopy, there is no means of determining ground cover using optical sensors.

DISCUSSION

Analysis of the prototype version of our snow-mapping algorithm, SNOMAP, has shown it to be effective in mapping snow cover on TM scenes in which a variety of surface covers is represented. SNOMAP provided more consistent results than were derived from a supervised-classification technique. Compared with a TM scene of the Sierra Nevada Mountains, mapped by spectral-mixture modeling, SNOMAP was 98% accurate in mapping snow in pixels that were at least 60% snow covered.

An estimate of the limitation, globally, in mapping snow-covered area due to dense forests will be developed in the pre-launch time frame. As land-cover maps improve, we will be able to determine how much of the land is covered by forests that are too dense to permit snow to be adequately mapped below using the current algorithm. It will be possible to apply a different algorithm to densely forested areas that will more accurately identify snow underneath forests.

Work is ongoing to determine if the thresholds currently used in SNOMAP will apply universally. If, for example, images acquired when the solar elevation is low require a different threshold setting, this can be

Table 4. Snow-Covered Area (SCA) in km^2 and Percentage of Full TM Scene Determined Using Supervised Versus SNOMAP Classification Techniques

	Supervised	*SNOMAP*	*Percentage of* change in SCA
	km^2 (percentage)	*km^2 (percentage)*	
GNP 14Mar91	6,450 (19.1)	10,631 (31.5)	−39.3
GNP 06Mar94	10,253 (30.3)	10,953 (32.4)	−6.4
GNP 09May94	4,126 (12.2)	4,006 (11.9)	2.9
Ch 29Sep92	12,841 (38.0)	16,021 (47.5)	−19.8
Vat 19Oct92	12,020 (35.6)	13,033 (38.6)	−7.8
MN 09Mar85	19,443 (57.6)	21,534 (63.8)	−9.7

GNP refers to Glacier National Park, Montana; Ch refers to the Chugach Mts., Alaska; Vat refers to Vatnajökull, Iceland; and MN refers to northern Minnesota. Percentage of change refers to the change in the amount of SCA mapped using the two different approaches for mapping snow cover, relative to the SNOMAP result.

accommodated in the algorithm. The next challenge in this ongoing research is to locate and analyze TM scenes that were acquired under conditions of low solar elevation.

The MODIS snow maps will complement the suite of planned MODIS products (Salomonson and Toll, 1991; Running et al., 1994). Land cover, surface albedo, sea ice cover, net-primary productivity, surface temperature, and other products will be available for intercomparison. SNOMAP can be applied using MODIS 1-km and 500-m resolution data, thus enabling both global- and regional-scale measurements to be made, though only 500-m daily and 7-day composite global maps will be produced as MODIS products. Two 250-m resolution bands will permit more detailed, but limited, mapping of regional snow-cover characteristics.

MODIS-derived global snow-cover data products will be available to use in general circulation models (GCMs) and will represent a consistent snow-cover data set for long-term climatology studies. Snow-cover data will also be available to use as input into regional-scale hydrological models to permit improved estimates of runoff, and for hydrological- and energy-balance modeling.

In September 1995 a MODIS snow and ice workshop was held at Goddard. An objective of the workshop was to seek advice from the snow and ice community on the MODIS snow product. There was considerable discussion and many excellent ideas were put forth. As a result of the workshop, the snow product will be modified in the pre-launch time frame so that it will better meet the needs of potential users. Thus, there are likely to be enhancements to the product in the next couple of years that are not discussed in this paper.

Advanced-classification techniques, currently being developed (Nolin et al., 1993), permit subpixel classification and improve the identification of fractional snow cover. It is likely that spectral-mixture modeling, or another advanced-classification technique that does not rely on thresholding, will be implemented after launch when we can "train" on the entire globe to select suitable endmembers for analysis. If a better snow-cover product can be obtained using advanced-classification techniques, then all data will be reprocessed in the post-launch time frame to provide an optimum product.

Outlook for the Future

The combined use of visible, near-infrared, and microwave sensors is likely to offer a better way to map snow extent and water equivalent in the future. Much work is already ongoing in this area (Chang et al., 1992b; Salomonson et al., 1995; Grody and Basist, in press). Because passive-microwave sensors are generally unaffected by cloud cover over snow-covered areas, it will be advantageous to use MODIS data in conjunction with Advanced Microwave Sounding Radiometer (AMSR) data to map daily snow extent and water equivalent. The AMSR may be flown on the EOS PM satellite along with MODIS early in the next century (personal communication, Claire Parkinson / GSFC). The spatial resolution of the passive-microwave data on the AMSR may be as good as 5 km, thus AMSR will be far more useful for mapping snow parameters than are the satellite-borne passive-microwave sensors of today, which have a maximum spatial resolution of about 15 km.

CONCLUSION

It is concluded that the planned MODIS snow-cover products will represent an advance over products presently available because the daily and weekly maps will be derived automatically using the unique capabilities of the MODIS at 500-m resolution (e.g., snow / cloud discrimination using spectral bands that are not available today and ability to derive spectral reflectance). Additionally, there will be snow-cover persistence statistics derived for each MODIS 500-m pixel globally from the weekly maps. Results also show that an automated-classification technique gives more consistent results

than does a supervised-classification technique. The SNOMAP algorithm will continue to evolve before and after the planned 1998 launch of MODIS and if more-advanced snow-cover mapping techniques emerge, then data will be reprocessed after launch. In short, the MODIS snow-cover products as part of a suite of MODIS products, will allow us to improve our ability to monitor and model key geophysical processes.

The authors would like to thank Walter Rosenthal / University of California at Santa Barbara, for discussions concerning results of fractional-snow mapping work; Janet Chien / General Science Corporation, Laurel, MD, for image processing of the TM data; and Tom Carroll of NOAA / National Hydrologic Remote Sensing Center, Minneapolis, Minnesota; Jim Foster / NASA / GSFC; and Anne Nolin / University of Colorado, Boulder, Colorado, for their reviews of the paper.

REFERENCES

Allen, T. R., and Walsh, S. J. (1993), Characterizing multitemporal alpine snowmelt patterns for ecological inferences, *Photogram. Eng. Remote Sens.* 59(10):1521–1529.

Bromwich, D. H., and Tzeng, R.-Y. (1994), Simulation of the modern arctic climate by the NCAR CCM1, *J. Climate* 7: 1050–1069.

Bunting, J. T. and d'Entremont, R. P. (1982), Improved cloud detection utilizing defense meteorological satellite program near infrared measurements, Air Force Geophysics Laboratory, Hanscom AFB, MA, AFGL-TR-82-0027, *Environmental Research Papers* No. 765, 91p.

Carroll, T. R. (1990), Operational airborne and satellite snow cover products of the National Operational Hydrologic Remote Sensing Center, *Proceedings of the Forty-seventh Annual Eastern Snow Conference*, June 7-8, 1990, Bangor, Maine, CRREL Special Report 90–44.

Carroll, T. R., Baglio, Jr., J. V., Verdin, J. P. and Holroyd, III, E. W. (1989), Operational mapping of snow cover in the United States and Canada using airborne and satellite data, *Proceedings of the 12th Canadian Symposium on Remote Sensing*, V.3, IGARSS '89, 10–14 July 1989, Vancouver, Canada.

Chang, A. T. C., Foster, J. L., and Rango, A. (1992a), The role of passive microwaves in characterizing snow cover in the Colorado River Basin, *Geojournal* 26.3:381–388.

Chang, A. T. C., Foster, J. L., Hall, D. K., Robinson, D. A., Pieji, L., and Meisheng, C. (1992b), The use of microwave radiometer data for characterizing snow storage in western China, *Ann. Glaciol.* 16:215–219.

Dozier, J. (1984), Snow reflectance from Landsat-4 thematic mapper, *I.E.E.E. Trans. Geosci. Remote Sens.* 22:323–328.

Dozier, J. (1989), Spectral signature of alpine snow cover from the Landsat Thematic Mapper, *Remote Sens. Environ.* 28 9–22.

Dozier, J., Schneider, S. R., and McGinnis, D. F., Jr. (1981), Effect of grain size and snowpack water equivalence on visible and near-infrared satellite observations of snow, *Water Resources Res.* 17:1213–1221.

Fleig, A. J., Hubanks, P. A., Storey, J. C., and Carpenter, L. (in press), An analysis of MODIS earth location errors, Version 2.0.

Foster, J. L. and Chang, A. T. C. (1993), Snow cover, In *Atlas of Satellite Observations Related to Global Change*, R. J. Gurney, C. L. Parkinson, and J. L. Foster (Eds.), Cambridge University Press, Cambridge, pp. 361–370.

Foster, J. L., Chang, A. T. C., Hall, D. K., and Rango, A. (1991), Derivation of snow water equivalent in boreal forests using microwave radiometry, *Arctic* 44 (Suppl. 1):147–152.

Foster, J. L., Chang, A. T. C., and Hall, D. K. (1994), Snow mass in boreal forests derived from a modified passive microwave algorithm, *Proceedings of the European Symposium on Satellite Remote Sensing*, Conference on Microwave Sensing for Forestry and Hydrology, Rome, Italy, September 1994.

Goodison, B. E., Rubinstein, I., Thirkettle F. W., and Langham, E. J. (1986), Determination of snow water equivalent on the Canadian Prairies using microwave radiometry, *IAHS* Publication No. 155, 163–173.

Grody, N. C. and Basist, A. (in press), Global identification of snowcover using SSM / I measurements.

Gutzler, D. S., and Rosen, R. D. (1992), Interannual variability of wintertime snow cover across the Northern Hemisphere, *J. Climate.* 5:1441–1447.

Hall, D. K., Foster, J. L., and Chang, A. T. C. (1982), Measurement and modeling of microwave emission from forested snowfields in Michigan, *Nordic Hydrol.* 13:129–138.

Hall, D. K., Foster, J. L., and Chang, A. T. C. (1992), Reflectance of snow as measured in situ and from space in subarctic areas in Canada and Alaska, *IEEE Trans. Geosci. Remote Sens.* V.30(3):634–637.

Hall, D. K., Foster, J. L., Chien, J. Y. L., and Riggs, G. A. (in press), Determination of actual snow cover using Landsat TM and digital elevation model data in Glacier National Park, Montana, *Polar Rec.*

Hallikainen, M. T., Jolma, P. A., and Hyyppa, J. M. (1988), Satellite microwave radiometry of forest and surface types in Finland, *IEEE Trans. Geosci. Remote Sens.* 26:622–628.

King, M. D., Kaufman, Y. K., Menzel, W. P., and Tanre, D. (1992), Remote sensing of cloud, aerosol, and water vapor properties from the Moderate Resolution Imaging Spectroradiometer (MODIS), *IEEE Trans. Geosci. Remote Sens.* 30: 2–27.

Kyle, H. L., Curran, R. J., Barnes, W. L., and Escoe, D. (1978), A cloud physics radiometer, *Third Conference on Atmospheric Radiation*, Davis, CA, pp. 107–109.

Markham, B. L., and Barker, J. L. (1986), Landsat MSS and TM post-calibration dynamic ranges, exoatmospheric reflectances and at-satellite temperatures, in *EOSAT Technical Notes*, No. 1, 3–8.

Matson, M., Roeplewski, C. F., and Varnadore, M. S. (1986), *An Atlas of Satellite-Derived Northern Hemisphere Snow Cover Frequency*, National Weather Service, Washington, DC, 75 pp.

Matson, M., (1991), NOAA satellite snow cover data, *Palaeogeog. and Paleoecol.* 90:213–218.

NOAA (National Oceanic and Atmospheric Administration), (1994), *Fifth Annual Climate Assessment 1993*, Climate Analysis Center, Camp Springs, Maryland, March 1994, 111 pp.

Nolin, A., Dozier, J., and Mertes, L. A. K. (1993), Mapping

alpine snow using a spectral mixture modeling technique, *Ann. Glaciol.* 17:121–124.

Rango, A. (Ed.), (1975), *Operational Applications of Satellite Snowcover Observations*, NASA SP-391, 430 pp.

Rango, A. (1993), Snow hydrology processes and remote sensing, *Hydrol. Proc.* 7:121–138.

Rango, A., and Martinec, J. (1982), Snow accumulation derived from modified depletion curves of snow coverage, *Symposium on Hydrological Aspects of Alpine and High Mountain Areas*, in Exeter, IAHS Publication No. 138, pp. 83–90.

Riggs, G. A., Hall, D. K., and Salomonson, V. V. (1994), A snow index for the Landsat Thematic Mapper and Moderate Resolution Imaging Spectroradiometer, *Proceedings of the International Geoscience and Remote Sensing Symposium*, IGARSS'94, 8–12 August 1994, Pasadena, CA, pp. 1942–1944.

Robinson, D. A., and Kukla, G. (1985), Maximum surface albedo of seasonally snow covered lands in the Northern Hemisphere, *J. Climate Appl. Meteorol.* 24:402–411.

Robinson, D. A. and Dewey, K. F. (1990), Recent secular variations in the extent of Northern Hemisphere snow cover, *Geophys. Res. Lett.* 17:1557–1560.

Robinson, D. A., Keimig, F. T., and Dewey, K. F. (1991), Recent variations in Northern Hemisphere snow cover, *Proceedings of the 15th Annual Climate Diagnostics Workshop*, Asheville, NC, NOAA, pp. 219–224.

Robinson, D. A., Dewey, K. F., and Heim, R. R., Jr. (1993), Global snow cover monitoring: An update, *Bull. Am. Meteorol. Soc.* 74:1689–1696.

Rosenthal, C. W. (1993), Mapping montane snow cover at subpixel resolution from the Landsat thematic mapper, M.A. thesis, Department of Geography, University of California at Santa Barbara, 70 pp.

Rossow, W. B. (1993), Clouds, In *Atlas of Satellite Observations Related to Global Change*, (R. J. Gurney, J. L. Foster, and C. L. Parkinson, Eds.), Cambridge University Press, Cambridge, England, pp. 141–163.

Running, S. W., Justice, C., Salomonson, V., et al. (1994), Terrestrial remote sensing science and algorithms planned for EOS / MODIS, *Int. J. Remote Sens.* 15(17):3587–3620.

Salomonson, V. V., and Toll, D. L. (1991), Execution phase (C / D) spectral band characteristics of the EOS moderate resolution imaging spectrometer-nadir (MODIS-N) facility instrument, *Adv. Space Res.* 11:231–236.

Salomonson, V. V. and Barker, J. L. (1992), EOS Moderate Resolution Imaging Spectroradiometer: Phase C / D status and comments on calibration and georeferencing approaches, *Proceedings of the 15th Annual AAS Guidance and Control Conference*, 8–12 February 1992, Keystone, Colorado, 1–14.

Salomonson, V. V., Toll, D. L., and Lawrence W. L. (1992), Moderate Resolution Imaging Spectroradiometer (MODIS) and observations of the land surface, *Proceedings of the International Geoscience and Remote Sensing Society Annual Meeting*, 26–29 May 1992, Houston, TX, pp. 549–551.

Salomonson, V. V., Hall D. K., and Chien, J. Y. L. (1995), Use of passive microwave and optical data for large-scale snow-cover mapping, *Proceedings of the Combined Optical-Microwave Earth and Atmospheric Sensing*, 3–6 April 1995, Atlanta, GA.

Steffen, K. (1987), Bidirectional reflectance of snow, In *Large Scale Effects of Seasonal Snow Cover*, B. E. Goodison, R. G. Barry, and J. Dozier, Eds. Proceedings of the IAHS Symposium held in Vancouver on 19–22 August 1987, IAHS, Vancouver, Canada, pp. 415–425.

Tiuri, M. and Hallikainen, M. (1981), Microwave emission characteristics of snow covered Earth surfaces measured by the Nimbus-7 satellite, *11th European Microwave Conference*, Amsterdam, September 1981, 233–238.

Townshend, J. R. G., Tucker, C. J. and Goward, S. N., (1993), Global vegetation mapping, In *Atlas of Satellite Observations Related to Global Change* R. J. Gurney, J. L. Foster and C. L. Parkinson, (Eds.), Cambridge University Press, London, England, pp. 301–311.

Tucker, C. J. (1979), Red and photographic infrared linear combinations for monitoring vegetation, *Remote Sens. Environ.* 8:127–150.

Tucker, C. J. (1986), Maximum normalized difference vegetation index images for sub-Saharan Africa for 1983–1985, *Int. J. Remote Sens.* 7:1383–1384.

Walsh, J. E., Jasperson, W. H., and Ross, B. (1985), Influences of snow cover and soil moisture on monthly air temperature, *Monthly Weather Rev.* 113:756–768.

Winther, J.-G. (1992), Landsat thematic mapper (TM) derived reflectance from a mountainous watershed during the snow melt season, *Nordic Hydrol.* 23:273–290.